

## **Supporting Information Text**

### **Materials and methods**

#### **CI users**

None of the participants experienced any complications during their CI surgery and no abnormalities were identified on post-operative X-ray. For all participants, all implantable electrodes were situated within the cochlea and post-operative impedances were within normal range on all electrodes. For one participant, activation of the device was delayed by one week due to an infection around the surgical site of incision. All participants were stimulated in monopolar configuration, and comfort and threshold levels were estimated for each electrode position by the clinical team according to standard clinical protocols.

#### **Testing conditions**

All stimuli were presented, and scored where appropriate, using the MATLAB<sup>®</sup> computing environment (Release 2014b, The MathWorks, Natick, MA). A centrally located Genelec 8030A loudspeaker was mounted immediately above and behind the visual display unit. The sound pressure level (SPL) of auditory stimuli was measured at the listening position with the participant absent using a Brüel & Kjær 2250 sound level meter and free-field microphone (Type 4189). A dense sound-absorbing screen was placed between the fNIRS equipment and the participant to attenuate the steady fan noise generated by the equipment. This resulted in a steady ambient noise level of 38 dB SPL (A-weighted). The fNIRS equipment remained switched on, although not recording, throughout behavioural testing. Prior to the commencement of each test, participants were provided with written instructions to ensure understanding and consistency of instructions given.

#### **Familiarisation runs**

During the fNIRS familiarisation session, one block of each of the conditions was presented. In order to avoid pre-exposure to the experimental stimuli, the familiarisation blocks comprised speech material (BKB sentences (39)) that were different to the material presented during the fNIRS measurements and the subsequent behavioural testing. Following each stimulation block, an example of the attentional control task was also presented. Similarly, BKB sentences were employed during the behavioural familiarisation run in order to avoid pre-exposure to the CUNY corpus.

## **Optode placement**

Together, the optode arrays comprised ten emitter and eight detector optodes with a fixed inter-optode distance of 30 mm, providing a penetration depth into the cortex of approximately 15 mm (40). This resulted in a total of 24 measurement channels (12 per hemisphere). Optode positioning was guided by the International 10-20 System (30) to promote consistency across participants and test sessions. Specifically, on each side, the lowermost source optode was placed as close as possible to the preauricular point, with the uppermost source optode aligned towards Cz. Consistency of optode positioning across test sessions at the individual level was further ensured by reference to photographs taken during the initial testing session.

To evaluate the consistency of optode positioning across individuals, the procedure was piloted on six adult volunteers who did not take part in the main experiment. After positioning the arrays as described above, the optode positions, plus anatomical surface landmarks, were recorded using the Hitachi ETG-4000's electromagnetic 3D Probe Positioning Unit. For each volunteer, the digitized optode positions were registered to a standard atlas brain (41) ('Colin27') using the AtlasViewer tool (31), allowing their locations to be visualized relative to underlying cortical anatomy. The standard deviation in the position of each optode was between 2.9 and 8.8 mm. Assessment of the mean optode positions suggested that the array provided good coverage of STC (Fig. S4).

## **Behavioural test of speech understanding**

The CUNY corpus was employed primarily due to its routine use as a clinical outcome measure by CI programmes across the UK. Additionally, this corpus was not presented during fNIRS scanning, thus helping to limit training effects within and across testing sessions.

## **Processing of fNIRS data**

Raw light intensity measurements were first converted to change in optical density (34). Wavelet motion correction was then performed to reduce the impact of motion artefacts on the fNIRS signal. Wavelet filtering can enhance data yield and has emerged as a favourable approach for use with fNIRS data (42). The HOMER2 `hmrMotionCorrectWavelet` function (based on (42)) was used which assumes that the wavelet coefficients have a Gaussian probability distribution and so applies a probability threshold to remove outlying wavelet

coefficients that are assumed to correspond to motion artefacts. A probability threshold was set to exclude coefficients lying more than 1.5 inter-quartile ranges below the first quartile or above the third quartile.

Following motion-artefact correction, a bandpass filter of 0.01–0.5 Hz was applied to reduce sources of physiological noise in the data including high-frequency cardiac oscillations, low-frequency respiration and blood pressure changes. The fNIRS signal was next converted into estimates of changes in HbO and HbR using the modified Beer-Lambert law with a default differential path-length factor of six (34). As bandpass filtering is unable to remove all physiological noise from fNIRS recordings (34), the haemodynamic signal separation method of (37) was also applied. This algorithm separates the fNIRS signal into estimates of the functional and systemic components, based on expected differences in the correlation between HbO and HbR in each component. Specifically, a positive correlation between changes in HbO and HbR is assumed in the systemic component, whereas a negative correlation is assumed in the functional component. The functional component of the signal was identified by the algorithm, extracted from the fNIRS signal and retained for further analysis.

### **Processing of behavioural data**

The arcsine transform ( $T$ ) was applied as follows:

$$T = \arcsine \sqrt{\frac{X}{N+1}} + \arcsine \sqrt{\frac{X+1}{N+1}}$$

The ‘asin’ function in Matlab was used to return the inverse sine (arcsine) for each value of  $X$ , where  $X$  represents the total number of words reported correctly and  $N$  represents the total number of words presented. This was then transformed linearly:

$$R = 46.47324337T - 23$$

where  $R$  indicates the resulting rationalised arcsine-transformed score (rationalised arcsine unit, RAU). This transformation extends the original percent correct scale outwards in both directions from 50%, creating bigger differences as the extremes of the range are approached. Consequently, this transformation makes the rationalised arcsine scale linear and additive in its proportions whilst producing values close to that of the original percentage scores (38).

### **Linear mixed model analysis**

Linear mixed models (LMMs) are able to give accurate estimates of the fixed effect of predictor variables whilst incorporating and accounting for the random effects that are often inherent in repeated-measures designs (43). Missing data were missing for reasons that were unrelated to the observed data values (i.e. attrition and unrelated medical condition). The LMMs were therefore conducted under the assumption that missing data were ‘missing at random’(43). Thus, the LMMs maximised the use of available data rather than entirely omitting subjects with missing data values from the analysis.

Due to the repeated measures design, ‘participant’ was specified as a variable to incorporate within-participant covariance into the fixed effect estimation. Furthermore, a random intercept effect and random effect of time were also specified to facilitate the estimation of the fixed effect of ‘group’ and ‘time’ whilst accounting for possible between-subject variability in overall fNIRS response amplitude and the trajectory of change over time.

### Legends for supporting figures

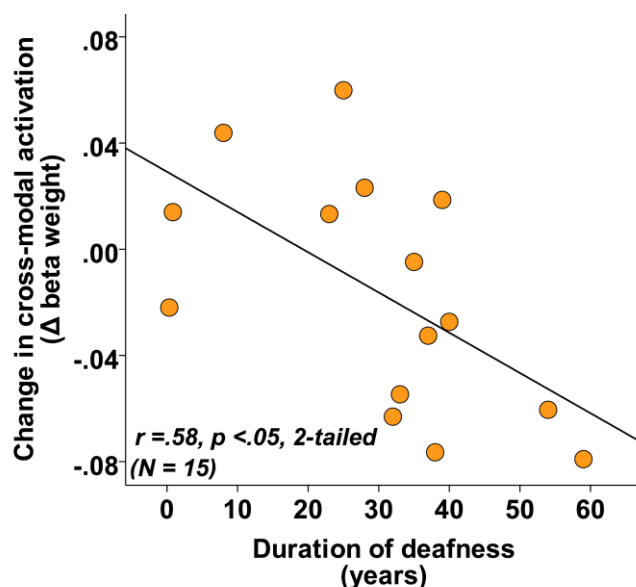


**Figure S1: Relationship between change in cross-modal bilateral STC activation and duration of deafness.** Change in cross-modal activation of bilateral STC by visual speech ( $\Delta$  beta weight; arbitrary units) from T0 to T1 is plotted against the duration of bilateral hearing loss prior to implantation (years), with regression line shown.

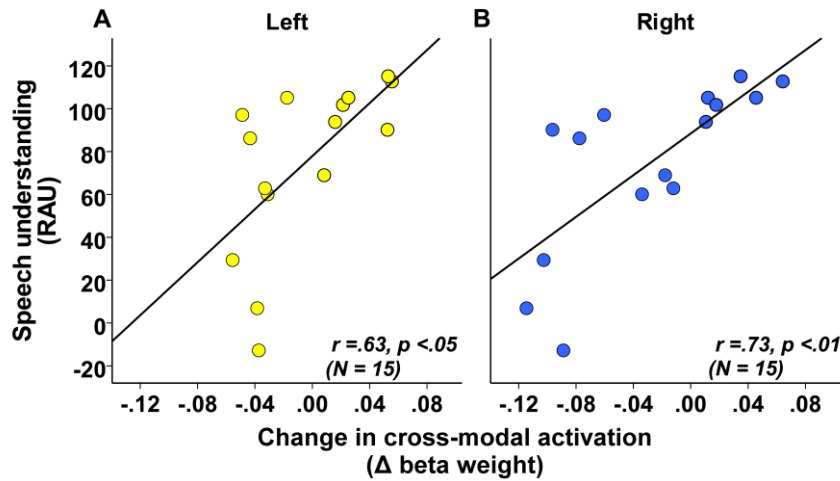


**Figure S2: Change in cross-modal activation of left and right STC and speech understanding.** Change in cross-modal activation of STC by visual speech ( $\Delta$  beta weight; arbitrary units) from T0 to T1 is plotted against speech understanding (RAU) at T1, with the regression line shown for (A) the left hemisphere, and (B) the right hemisphere.

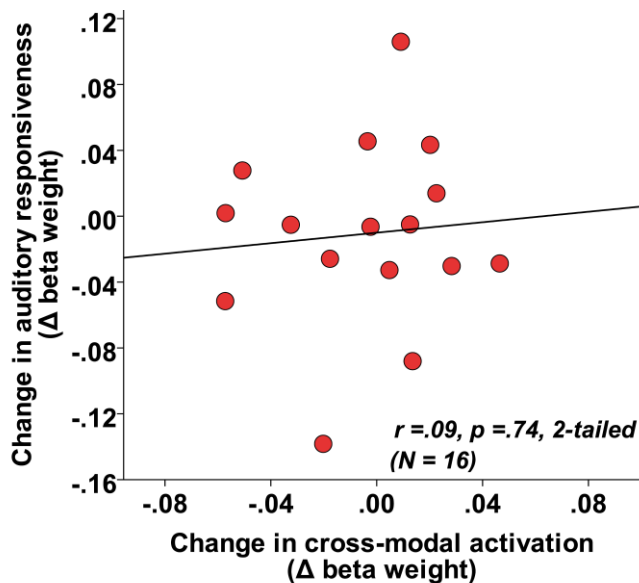


**Figure S3: Change in cross-modal STC activation and auditory responsiveness in control subjects.** Change in cross-modal activation of bilateral STC by visual speech from T0 to T1 ( $\Delta$  beta weight; arbitrary units) is plotted against change in bilateral auditory responsiveness from T0 to T1 with the regression line shown.

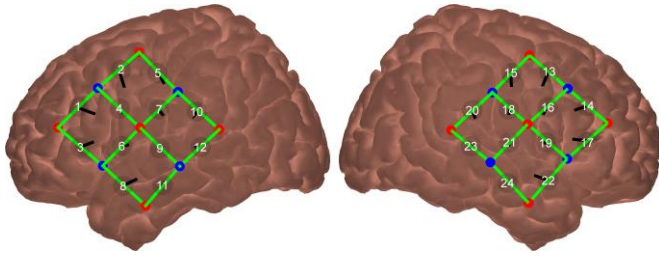


**Figure S4: Mean position of fNIRS optodes and measurement channels**

Measurement channels are labelled numerically, source optodes are indicated in red and detector optodes are indicated in blue.